hMre11 and hRad50 Nuclear Foci Are Induced during the Normal Cellular Response to DNA Double-Strand Breaks†

RICHARD S. MASER,[1] KIRSTEN J. MONSEN,[1] BENJAMIN E. NELMS,[2] AND JOHN H. J. PETRINI[1]*

*Laboratory of Genetics[1] and Department of Medical Physics,[2] University of
Wisconsin Medical School, Madison, Wisconsin 53706*

We previously identified a conserved multiprotein complex that includes hMre11 and hRad50. In this study, we used immunofluorescence to investigate the role of this complex in DNA double-strand break (DSB) repair. hMre11 and hRad50 form discrete nuclear foci in response to treatment with DSB-inducing agents but not in response to UV irradiation. hMre11 and hRad50 foci colocalize after treatment with ionizing radiation and are distinct from those of the DSB repair protein, hRad51. Our data indicate that an irradiated cell is competent to form either hMre11-hRad50 foci or hRad51 foci, but not both. The multiplicity of hMre11 and hRad50 foci is much higher in the DSB repair-deficient cell line 180BR than in repair-proficient cells. hMre11-hRad50 focus formation is markedly reduced in cells derived from ataxia-telangiectasia patients, whereas hRad51 focus formation is markedly increased. These experiments support genetic evidence from *Saccharomyces cerevisiae* indicating that Mre11-Rad50 have roles distinct from that of Rad51 in DSB repair. Further, these data indicate that hMre11-hRad50 foci form in response to DNA DSBs and are dependent upon a DNA damage-induced signaling pathway.

Certain intrinsic programs in eukaryotic organisms, such as meiotic and mitotic recombination, mating type switching, and assembly of antigen receptor genes, involve the generation of DNA double-strand breaks (DSBs) (63, 73, 78). DNA DSBs are also caused by a variety of extrinsic factors, including exposure to ionizing radiation and genotoxic chemicals (19). Proteins that mediate DNA DSB repair are required for both intrinsic DNA recombination processes and the repair of extrinsically induced DNA damage. Thus, DSB repair deficiency results in sensitivity to DNA DSB-inducing agents and impairs meiotic and mitotic DNA recombination processes (21, 59). In addition, the failure to repair DNA DSBs can lead to the loss of genetic information by mutation, chromosome loss, or rearrangement and, in some instances, to cell death (29, 51).

In both *Saccharomyces cerevisiae* and mammalian cells, recombinational repair of DSBs occurs either by homologous recombination or by nonhomologous end joining (9, 24, 50, 64, 68). The *RAD52* epistasis group (*RAD50-RAD57, RAD59, MRE11*, and *XRS2*) is largely responsible for DSB repair in yeast (1, 5, 21, 30). Mutations in these genes cause profound recombination defects as well as sensitivity to DSB-inducing agents. The *RAD52* epistasis group can be subdivided into two subgroups according to specific functions in meiotic and mitotic recombination. In mitotic cells, *S. cerevisiae RAD51* (*ScRAD51*), *ScRAD52*, *ScRAD54*, *ScRAD55*, and *ScRAD57* comprise one subgroup, which mediates homologous recombination (21), whereas *ScRAD50*, *ScMRE11*, and *ScXRS2* mediate nonhomologous end joining (50, 68, 77).

We recently reported the identification of the human *MRE11* and *RAD50* homologs (15, 60). Mammalian homologs have also been identified for *RAD51*, *RAD52*, and *RAD54* (7,

34, 71, 72). Sequence homology between the yeast and human *RAD52* epistasis group proteins, as well as the conservation of an Mre11-Rad50 complex in human cells (15), suggests that certain mechanistic functions must also be conserved. Thus, human Mre11 (hMre11) and hRad50, like ScMre11 and ScRad50, are likely to function in nonhomologous end joining, the predominant mode of recombinational DNA repair in mammalian cells (9, 44). The role of the DNA-PK$_{CS}$–Ku complex in this mode of repair is well established (32, 78), but demonstration of functional interaction between the hMre11-hRad50 protein complex and the DNA-PK$_{CS}$–Ku complex awaits further study.

Direct examination of individual cells following genotoxic stress offers a powerful way to analyze the effects of DNA damage and its repair (14, 54). The identification of DNA repair proteins has provided molecular probes that, when combined with cytological assays, have yielded insight into the roles of the proteins in DNA metabolism. In this regard, immunofluorescence studies of DNA ligase I (49), ScRad51 and hRad51 (8, 41, 62, 75), and hMsh1 (6) have provided important information. Similarly, immunofluorescence assays of hRad51 (23), xeroderma pigmentosum type G protein (58), and proliferating cell nuclear antigen (48, 76) in the DNA damage response have implicated these proteins in the repair of particular classes of DNA damage.

We used immunofluorescence to examine the response of hMre11 and hRad50 to DNA-damaging agents. hMre11 and hRad50, like hRad51 (23), exhibit a dynamic redistribution within the nucleus following treatment with agents that induce DNA DSBs. hMre11 and hRad50 ionizing radiation-induced foci (IRIF) colocalize, suggesting that induced foci consist of hMre11-hRad50 protein complexes (15). hRad51 and hMre11 foci do not colocalize and do not form in the same nuclei, consistent with their independent roles in DSB repair. We found that the formation of IRIF is dependent on the genetic background of the cells examined. The hMre11-hRad50 IRIF response is enhanced in the DNA DSB repair-deficient cell line 180BR. In contrast, the IRIF response is drastically re-

duced in cells with mutations in the *ATM* gene. The ATM protein mediates signaling functions in the cellular DNA damage response which appear to be important in cell cycle arrest as well as in the repair of chromosomal damage (13, 52, 57). These results suggest that the hMre11-hRad50 protein complex functions in DNA DSB repair and that this function is regulated by a previously identified signal transduction pathway.

MATERIALS AND METHODS

Cell lines. IMR90 primary diploid fibroblasts were obtained from the American Type Culture Collection and were used at passages 10 to 15, with equivalent results. 37Lu primary fibroblasts were also obtained from the American Type Culture Collection and used at passages 3 to 7. 180BR primary fibroblasts were obtained from C. Arlett and were used at passages 8 to 13. GM00637G normal simian virus 40 (SV40)-transformed fibroblasts and the SV40-transformed ataxia-telangiectasia (AT) cell lines GM09607A and GM05849B were obtained from the Coriell Institute for Medical Research. M059J and M059K cells were obtained from M. J. Allalunis-Turner. Primary fibroblasts were grown in Dulbecco modified Eagle medium–10% fetal calf serum (FCS), and SV40-transformed fibroblasts were grown in Dulbecco modified Eagle medium–5% FCS–5% Cosmic Calf serum (Hyclone, Logan, Utah). K562 CML cells (provided by Peggy Farnham) were grown in RPMI 1640–10% Cosmic Calf serum–1% Pen-Strep–2 mM L-glutamine. All cells were maintained at 37°C in a 5% CO_2–95% air humidified environment. All cells routinely tested negative for mycoplasmas with the MycoTect kit (Gibco, Grand Island, N.Y.).

Irradiation and drug treatment. Cells were irradiated in a Mark I ^{137}Cs source at a dose rate of approximately 2.5 Gy/min. UV irradiation was done in a UV cross-linking instrument (Stratagene, La Jolla, Calif.). For drug treatment, cells were exposed to etoposide dissolved as a 50% solution in dimethyl sulfoxide (DMSO) or an equivalent amount of DMSO alone (both from Sigma, St. Louis, Mo.) in growth medium for 1 h and then washed twice with phosphate-buffered saline (PBS) before replacement with drug-free medium.

Cell cycle analysis. Cell cycle analysis was performed as described previously with slight modifications (61) to retain apoptotic cells. Log-phase cells grown on 60-mm-diameter dishes were either untreated ($t = 0$ h) or irradiated and fixed at various time points after irradiation. Cells were trypsinized, collected along with the used medium, and washed once in PBS. The resulting cell pellet was suspended in 100 µl of 150 mM NaCl–10 mM Tris-HCl (pH 7.0) to which 900 µl of ice-cold 95% ethanol was added dropwise. Fixed cells were stored at 4°C at least overnight, pelleted, and washed in phosphate-citrate buffer (192 mM Na_2HPO_4, 4 mM $Na_3C_6H_5O_7$). The final washed pellet was stained in a solution containing 33 µg of propidium iodide per ml, 0.3 mg of RNase A per ml, and 0.2% Nonidet P-40 in PBS. Cell cycle analysis was performed on an EPICS Profile II flow cytometer (Coulter, Miami, Fla.).

Antibodies. Affinity purification of hMre11 and hRad50 rabbit antisera has been described previously (15). The fluorescent dye Texas Red was directly conjugated to affinity-purified anti-hMre11 by using a Fluoreporter kit (Molecular Probes, Eugene, Oreg.). Rabbit antiserum directed against hRad51 was a gift from Charles Radding (Yale University).

Immunofluorescence. Fibroblasts were seeded on Teflon-coated six-well slides (Cel-Line Associates, Newfield, N.J.) and allowed to adhere for at least 2 days prior to each experiment. Cells were irradiated or drug treated on slides, fixed at various time points in ice-cold methanol for 20 min at −20°C, and then permeabilized in ice-cold acetone for 10 s. Following fixation, slides were washed three times for 5 min each in PBS and blocked in 10% FCS–PBS for 1 h at room temperature. Slides were incubated for 1 h at 37°C with hMre11 (1:150 dilution), hRad50 (1:150 dilution), or hRad51 (1:400 dilution) primary rabbit antiserum, followed by fluorescein isothiocyanate (FITC)-conjugated goat anti-rabbit secondary antiserum (1:200 dilution) (Pierce, Rockford, Ill.) for 1 h at 37°C. All antisera were diluted in 1% bovine serum albumin–PBS. Slides were counterstained with 0.1 µg of DAPI (4′,6-diamidino-2-phenylindole) per ml for 1 min, mounted in antifade solution {2.3% DABCO (1,4-diazabicyclo[2.2.2]octane), 0.1 M Tris-HCl (pH 8.0), 90% glycerol}, and viewed via epifluorescence microscopy. After each blocking or antibody incubation step described above, slides were washed in PBS three times for 5 min.

For studies involving Texas Red-conjugated anti-hMre11, detection was performed as described above, followed by a 1-h blocking step as described above with the addition of a 1:100 dilution of rabbit serum. The slides were washed with PBS and incubated with Texas Red-conjugated anti-hMre11 (diluted 1:200) prior to counterstaining and mounting as described above. Differential staining observed with hRad50 and hRad51 antisera in combination with the Texas Red-conjugated hMre11 antiserum (see below) demonstrates the specificity of this staining method.

IRIF quantification and image capture. Foci were scored by eye at a magnification of ×600. At least 200 nuclei per time point were examined for each antiserum. A nucleus was considered positive for hMre11 or hRad50 IRIF if it contained at least five discernible foci. Nuclei containing fewer than five foci were scored as negative; positive nuclei were further categorized as those with 5
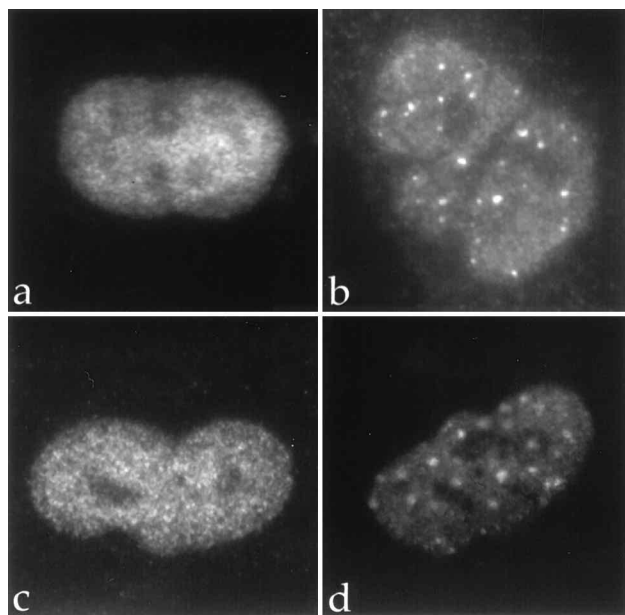

FIG. 1. hMre11 and hRad50 form nuclear foci following treatment with ionizing radiation. IMR90 primary human fibroblasts were seeded onto glass slides and either left untreated (a and c) or irradiated with 12 Gy (b and d) and fixed 8 h postirradiation (see Materials and Methods). Cells were then stained with anti-hMre11 (a and b) or anti-hRad50 (c and d) antiserum followed by FITC-conjugated goat anti-rabbit antiserum as described in Materials and Methods.

to 20 foci or >20 foci. In Fig. 6, positive nuclei were categorized as having 5 to 30 foci or >30 foci. For hRad51, a nucleus was considered positive if it contained at least 10 foci. Nuclear antibody staining was confirmed in each case with DAPI. Images were captured by using a cooled charge-coupled device (CCD) camera (Princeton Instruments, Trenton, N.J.), and grayscale images were processed by using Photoshop 4.0 (Adobe, San Jose, Calif.). Although images were captured with a CCD camera, all foci were readily observable by eye.

Comet assays. Cells were treated with etoposide or DMSO or were irradiated with 12 Gy or mock irradiated, trypsinized, and embedded in 1.5 ml of 1% agarose to yield a final density of approximately 10^4 cells/slide. Neutral comet assays were then performed as described previously (55). Comets were viewed under a final magnification of ×400, and images were captured with a CCD camera. Image acquisition and analysis were carried out with software written by one of us (B.E.N.). Percent DSBs remaining was calculated from tail moment values by using the formula (tail moment at 8 h − control tail moment)/(initial tail moment − control tail moment) × 100. Inquiries about the software should be directed to B.E.N. (e-mail, benelms@students.wisc.edu).

Immunoblotting, immunoprecipitation, and metabolic labeling. Immunoblot analyses with hMre11 and hRad50 antisera were carried out as described previously (15). For metabolic labeling, irradiated (12 Gy) and mock-irradiated cells were labeled at 2 h postirradiation with 80 µCi of [^{35}S]methionine (EasyTag; NEN, Boston, Mass.) per ml for 6 h longer and then harvested for immunoprecipitation analyses as described previously (15). Immunoprecipitates were fractionated on sodium dodecyl sulfate–7% polyacrylamide gels. Gels were then fixed for 20 min in 30% methanol–10% acetic acid, incubated in 1 M Na salicylate for 20 min, and autoradiographed at −80°C. Autoradiograms were scanned and processed as previously described (15).

RESULTS

hMre11 and hRad50 form nuclear foci in response to ionizing radiation. We have shown that steady-state levels of hRad50 and hMre11 proteins remain unchanged after gamma irradiation when assayed by immunoblotting (see Fig. 8a) (15, 45). We used immunofluorescence to investigate whether ionizing radiation induced alterations in the subcellular distribution of hMre11 and hRad50 in the human fibroblast cell line IMR90. Both hMre11 and hRad50 are abundant proteins that are uniformly distributed in the nuclei of unirradiated cells (Fig. 1a and c), with the exception of nucleoli. Following
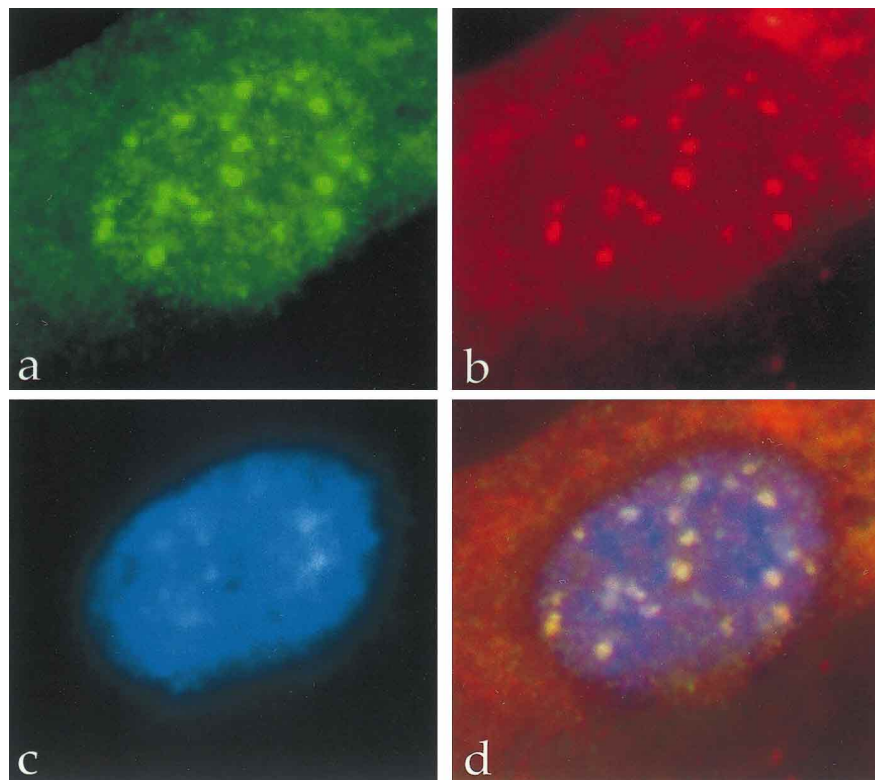
FIG. 2. hMre11 and hRad50 IRIF colocalize. 180BR primary human fibroblasts were irradiated with 8 Gy and fixed at 8 h postirradiation. Cells were stained with anti-hRad50 followed by Texas Red-conjugated anti-hMre11 (see Materials and Methods). Images of the same nucleus were captured under FITC (hRad50) (a), Texas Red (hMre11) (b), and DAPI (chromatin) (c) filters and merged (d) in Adobe Photoshop 4.0.

gamma irradiation, both hMre11 and hRad50 formed discrete nuclear foci (Fig. 1b and d), which are referred to as IRIF. Nuclear fluorescence was not observed in cells stained either with preimmune serum or with hMre11 antiserum that had been previously incubated with bacterially produced hMre11 protein (data not shown). DAPI counterstaining of irradiated cells indicated that IRIF-containing nuclei were not grossly aberrant and did not show signs of apoptosis (see Fig. 2c and 3c and f). Flow cytometric analyses of IMR90 cultures irradiated in parallel did not detect a significant population of apoptotic cells (data not shown).

hMre11 and hRad50 IRIF formation was also observed in the primary fibroblast cell line 37Lu, the glioblastoma cell lines M059J and M059K (2), HeLa cells (data not shown), and the SV40-transformed fibroblast cell line GM637 (see Fig. 7a).

hMre11 and hRad50 IRIF colocalize. We previously showed that hMre11 and hRad50 coimmunoprecipitate with three other proteins from human cell extracts (15). We found that the apparent stoichiometry and composition of the immunoprecipitated hMre11-hRad50 protein complex were not altered in extracts prepared from irradiated cells (see Fig. 8b). Accordingly, we used immunofluorescence to ask whether hMre11 and hRad50 IRIF colocalize. Immunofluorescence analysis of irradiated 180BR fibroblasts was performed with anti-hRad50 antiserum followed by FITC-conjugated goat anti-rabbit antiserum to detect bound antibody. Slides were washed, treated with blocking solution, and stained with Texas Red-conjugated anti-hMre11 antiserum. Images of nuclei were first captured with FITC filters (hRad50) (Fig. 2a), and then images of the same nuclei were captured with the Texas Red (hMre11) (Fig. 2b) and DAPI (chromatin) (Fig. 2c) filter sets. Merging of the

three images revealed that hMre11 and hRad50 IRIF colocalize within the nucleus (Fig. 2d). Colocalization of hMre11 and hRad50 IRIF has also been observed in IMR90 and 37Lu fibroblasts (data not shown).

The human Rad51 homolog, hRad51, has also been shown to form nuclear foci following DNA damage (23). We determined that hMre11 and hRad51 IRIF do not colocalize. Irradiated IMR90 fibroblasts were stained with anti-hRad51 antiserum and Texas Red-conjugated anti-hMre11 antiserum, as described above. Contrary to the results we obtained with anti-hRad50 and Texas Red-conjugated anti-hMre11 antisera, we observed distinct localization patterns for hRad51 and hMre11 nuclear foci (Fig. 3). Nuclei that contain hRad51 foci (Fig. 3a) did not contain hMre11 IRIF (Fig. 3b). Conversely, nuclei positive for hMre11 IRIF (Fig. 3e) did not contain hRad51 foci (Fig. 3d). In two independent experiments (792 nuclei examined), 123 nuclei were hRad51 IRIF positive, 236 nuclei were hMre11 IRIF positive, and none were positive for both types of IRIF. Therefore, irradiated fibroblasts that contained nuclear foci were positive for either hMre11 foci or hRad51 foci, but not both.

hMre11 and hRad50 IRIF are specific to DNA DSBs and form in a dose-dependent manner. Based on the involvement of yeast Mre11 and Rad50 in DSB repair and the lack of hMre11-hRad50 foci in unirradiated cells, we postulated that hMre11 and hRad50 IRIF were formed specifically in response to ionizing-radiation-induced DNA DSBs. Ionizing radiation has been shown to induce DNA DSBs in a dose-dependent, linear fashion (43, 53). We examined the dose dependence of hMre11-hRad50 IRIF formation in IMR90 cells. Cells were irradiated with 4, 8, or 12 Gy and evaluated at
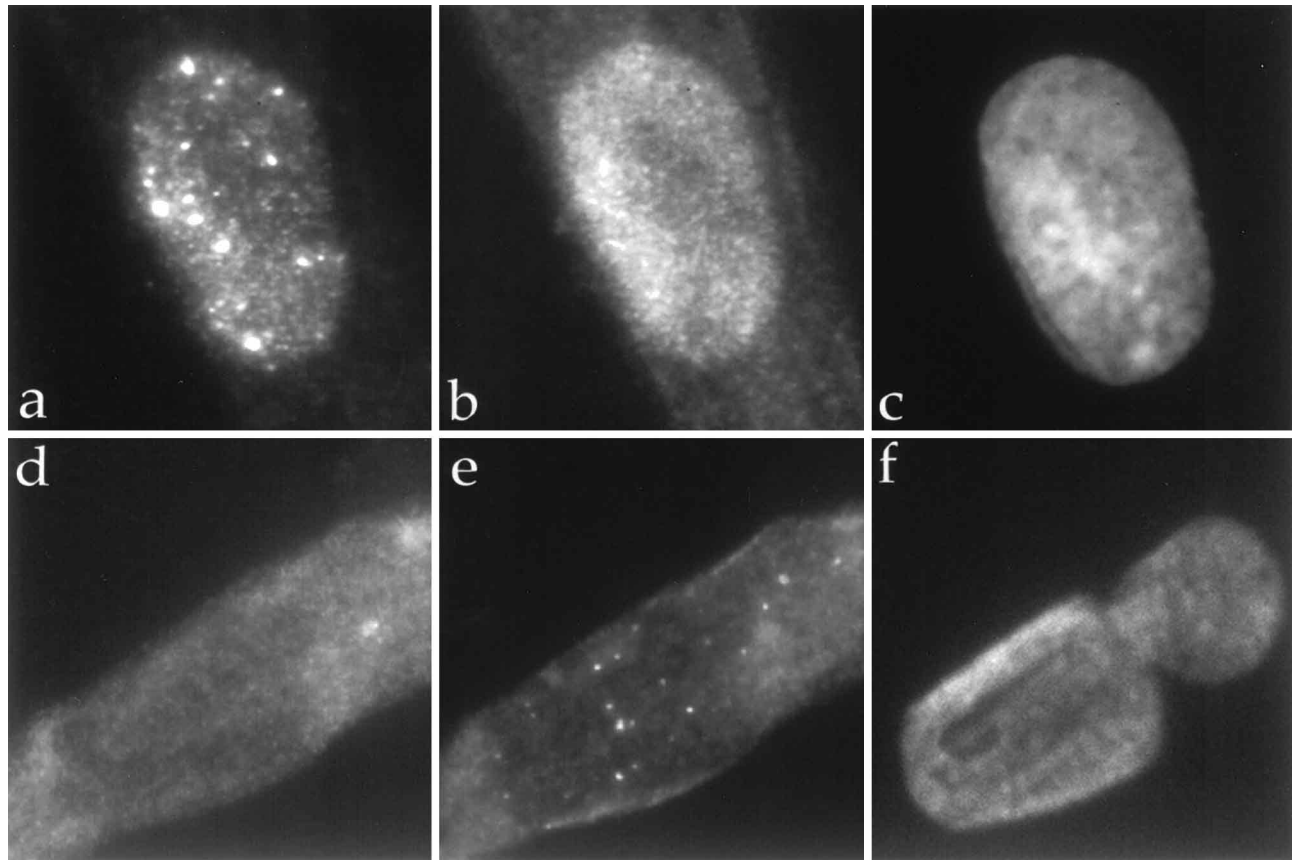
FIG. 3. hRad51 and hMre11 foci do not colocalize. IMR90 primary fibroblasts were irradiated with 12 Gy and fixed at 8 h postirradiation. Cells were then stained with anti-hRad51 followed by Texas Red-conjugated anti-hMre11 (see Materials and Methods). Images of nuclei were captured under FITC (hRad51) (a and d), Texas Red (hMre11) (b and e), and DAPI (chromatin) (c and f) filters. The images in panels a to c are of the same nucleus, as are those in panels d to f. hRad51 immunostaining was negligible in cells without nuclear foci, as reported previously (23).

8 h postirradiation. Nuclei were then scored for the number of observed hMre11 IRIF and placed in three categories: less than 5 (negative), 5 to 20, or >20 IRIF per nucleus. We found that the mean number of IRIF in the 5-to-20 class increased with the radiation dose (Fig. 4), as did the number of nuclei that fell into the >20 class (see Fig. 4 legend). An average of 6 IRIF per positive nucleus were observed at a dose of 4 Gy, and this increased to an average of over 12 IRIF per positive nucleus after 12 Gy. The percentage of nuclei that contained hMre11 IRIF also increased with the dose (Fig. 4), from less than 10% after 4 Gy to over 50% after 12 Gy.

We analyzed the response of hMre11 and hRad50 to other DNA-damaging agents to define the types of lesions that lead to IRIF formation. IMR90 fibroblasts were treated with the topoisomerase II inhibitor etoposide, a potent inducer of DNA DSBs (11, 70). Etoposide treatment (100 µg/ml) induced the formation of hMre11 foci indistinguishable from IRIF; 28% of nuclei examined were positive for foci at 8 h posttreatment (Table 1). Control cells treated with DMSO alone did not exhibit foci. We used the neutral comet assay (55) to show that this etoposide dose induced DNA DSBs and that 69% of these breaks remained unrepaired at 8 h posttreatment (Table 1). In contrast to ionizing radiation and etoposide treatment, no hMre11 or hRad50 foci were observed following UV irradiation at a dose of 16 J/m^2 (data not shown). This evidence suggests that hMre11-hRad50 IRIF form specifically in response to DNA DSBs.
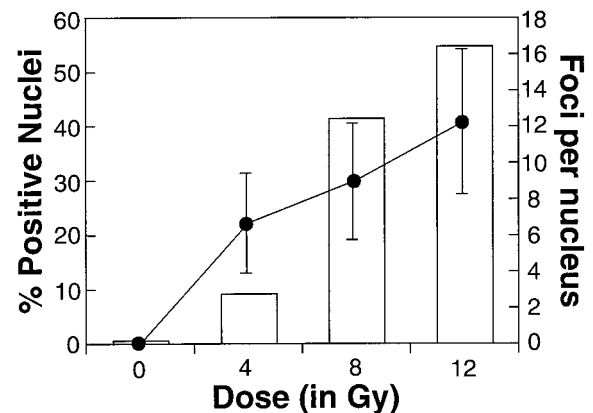

FIG. 4. IRIF formation is dose dependent. Log-phase IMR90 fibroblasts were irradiated with the indicated dose, fixed at 8 h following treatment, and stained with anti-hMre11 (see Materials and Methods). Nuclei were then scored for the presence of IRIF as described in Materials and Methods. Bars indicate the percentage of IRIF-positive nuclei (those with ≥5 foci; left axis), plotted versus radiation dose. Total number of nuclei examined for each dose: 0 Gy, 1,009; 4 Gy, 317; 8 Gy, 470; 12 Gy, 409. For the line graph, positive nuclei were separated into two classes: I, 5 to 20 foci/nucleus, and II, >20 foci/nucleus. The mean number of foci in class I was plotted (right axis) versus radiation dose. Error bars represent one standard deviation. For each dose, class II nuclei (not shown) represent 8, 34, and 45% of the total number of positive nuclei for 4, 8, and 12 Gy, respectively.

TABLE 1. DNA damage and IRIF formation

Cell line	% Initial DSBs remaining following treatment[b] (% hMre11 IRIF-positive nuclei[a])		
	DMSO	Etoposide	12 Gy of IR[c]
IMR90	0 (<1)	69 ± 16 (28)	12 ± 18 (45)
180BR	—[d]	—	100 ± 18 (45)
GM637	—	—	<1 ± 15 (24)
GM9607	—	—	48 ± 13 (24)

[a] Percentage of nuclei with five or more foci at 8 h after treatment.
[b] Determined by neutral comet assay at 8 h after treatment (see Materials and Methods). Results are means ± standard deviations.
[c] IR, ionizing radiation.
[d] —, not determined.

We determined the time course of IRIF formation following exposure to ionizing radiation. Log-phase IMR90 fibroblasts were irradiated with 12 Gy and fixed at 4, 8, and 24 h postirradiation. Independent slides were stained for hMre11 or hRad50. The percentage of nuclei with hMre11 and hRad50 IRIF increased to a maximum of greater than 60% at 8 h postirradiation, with a subsequent decrease in the percentage of IRIF-positive cells by 24 h (Fig. 5). Similar kinetics have been observed in other DSB repair-proficient cells (see below). We also examined the kinetics of hRad51 ionizing-radiation-induced foci (Fig. 5) and found that 32% of nuclei were positive for hRad51 foci at 4 and 8 h. These results were similar to those reported previously (23) but distinct from those for hMre11 and hRad50.

The hMre11-hRad50 IRIF response is altered in DNA DSB repair-deficient and cell cycle checkpoint mutant cells. We tested whether hMre11 and hRad50 IRIF formation was altered in the cell line 180BR, which is acutely sensitive to the effects of ionizing radiation (4). Due to a defect in the ability to repair DNA DSBs, the half-life of DSBs is extended in 180BR relative to that in repair-proficient cells (3). We tested whether

FIG. 6. Multiplicity of hMre11 and hRad50 IRIF in 180BR. Log-phase 180BR fibroblasts were irradiated with 12 Gy and fixed at 8 h postirradiation as described in Materials and Methods. Cells were then stained for either hMre11 or hRad50 and scored for IRIF as described in Materials and Methods. Positive nuclei were categorized as having either 5 to 30 IRIF or >30 IRIF. IMR90 cells from the 8-h time point in Fig. 5 were scored for IRIF similarly. Dark bars, hMre11, 5-30 foci; cross-hatched bars, hMre11, >30 foci; light bars, hRad50, 5 to 30 foci; hatched bars, hRad50, >30 foci. For 180BR, 243 and 281 total nuclei were scored for hRad50 and hMre11 IRIF, respectively.

the persistence of DNA DSBs in this cell line would alter the hMre11-hRad50 IRIF response. The multiplicity of IRIF in 180BR cells was increased for both hMre11 and hRad50 (Fig. 6), as measured by the number of IRIF observed in positive nuclei. Whereas only 12% of IMR90 cells that were positive for IRIF at 8 h after 12 Gy had greater than 30 foci per positive nucleus, 77% of 180BR cells at the equivalent time and dose exhibited greater than 30 foci per positive nucleus. Neutral comet assays carried out on irradiated 180BR cells confirmed that the majority of initial DSBs were unrepaired at 8 h postirradiation (Table 1). In contrast, greater than 90% of the initial DSBs were repaired by 8 h in IMR90 fibroblasts. Immunoblotting and immunoprecipitation analyses revealed that hMre11 and hRad50 expression and interaction appeared normal in 180BR cells and were unchanged with ionizing radiation (see Fig. 8a; data not shown). Consistent with the previously observed exclusivity of hMre11-hRad50 and hRad51 IRIF formation, the percentage of hRad51 IRIF-positive nuclei was reduced in 180BR relative to that in IMR90 (data not shown).

We also examined IRIF formation in cell lines derived from patients with the disease AT. Cells from AT patients have mutations in the *ATM* gene, which encodes a PI-3-like protein kinase (33, 36, 66). *ATM* mutant cells do not appear to be DSB repair deficient per se; rather, they appear to be deficient in signaling the presence of DNA damage. As a result, AT cells exhibit radioresistant DNA synthesis and are sensitive to killing by ionizing radiation (26, 38, 46, 56). To examine the dependence of hMre11 and hRad50 IRIF formation on the ATM-controlled response to DNA damage, we compared the kinetics of hMre11 and hRad50 IRIF formation in two SV40-transformed AT cell lines, GM5849 and GM9607, to those in the SV40-transformed normal human cell line GM637. When stained independently for either hMre11 or hRad50, IRIF-positive nuclei were observed in 25% of the GM637 cells examined at 10 h after 12 Gy, whereas the hMre11 and hRad50 response in both AT cell lines was drastically reduced (Fig. 7a). No more than 4% of nuclei were positive for hRad50 IRIF at any time in either AT cell line tested. For hMre11, we observed a maximum of 6.8% of nuclei that contained hMre11 IRIF in
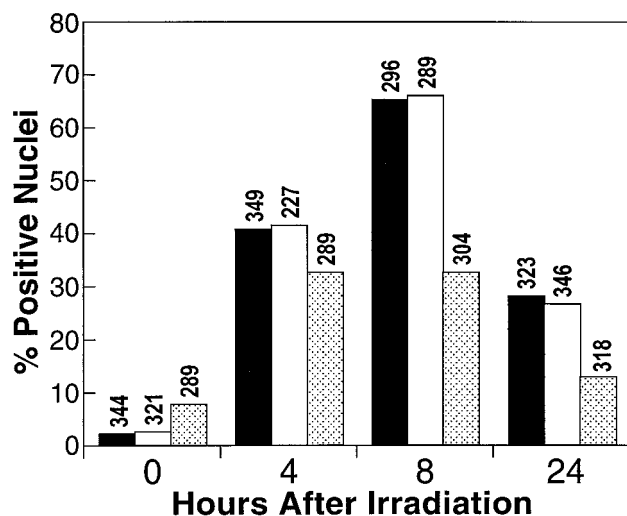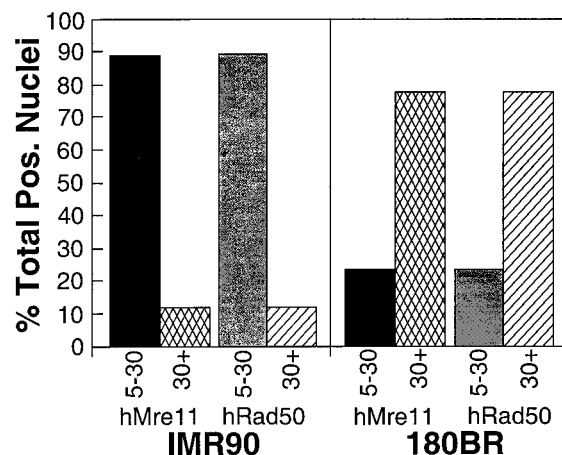

FIG. 5. Kinetics of IRIF formation. Log-phase IMR90 fibroblasts were either untreated ($t = 0$) or irradiated with 12 Gy and fixed at the indicated times postirradiation. Cells were then stained independently for either hMre11, hRad50, or hRad51 and scored for the presence of IRIF (see Materials and Methods). The percentage of IRIF-positive nuclei (≥5 foci for hMre11 or hRad50; ≥10 foci for hRad51) was plotted versus time after irradiation. Dark bars, hRad50; light bars, hMre11; stippled bars, hRad51. The total number of nuclei examined at each time for each antibody is indicated.
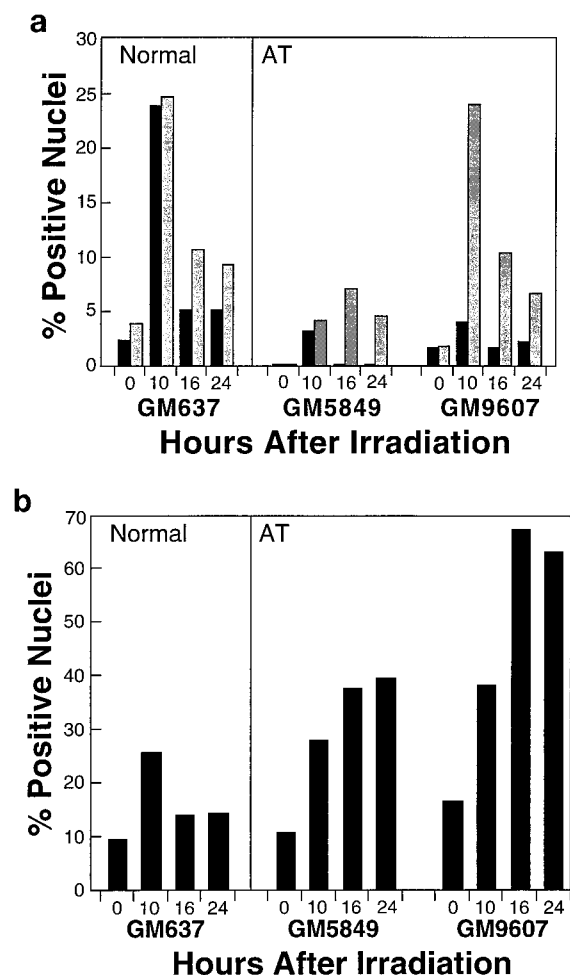
FIG. 7. Time course of IRIF formation in SV40-transformed normal and AT cell lines. (a) Log-phase normal (GM637) and AT (GM5849 and GM9607) cells were irradiated with 12 Gy or untreated ($t = 0$) and fixed at the indicated times after irradiation. Cells were then stained independently with anti-hMre11 or anti-hRad50 and scored for IRIF (see Materials and Methods). The percentage of IRIF-positive cells was plotted versus time after irradiation. Dark bars, hRad50; light bars, hMre11. Over 300 nuclei from each cell line were examined at each time point for both antibodies. (b) Time course of hRad51 IRIF formation. GM637, GM5849, and GM9607 cells were irradiated as described above, stained with anti-hRad51, and scored for hRad51 IRIF as indicated in Materials and Methods. The percentage of hRad51 focus-positive nuclei was plotted versus time after irradiation. Over 300 nuclei from each cell line were examined per time point.

amine the kinetics of hRad51 focus formation in AT cells. GM637 cells exhibited a normal hRad51 response following gamma irradiation (Fig. 7b) (23). At 24 h postirradiation, only 10% of GM637 cells were positive for hRad51 foci. However, in contrast to hMre11 and hRad50 IRIF formation, 45 and 75% of the GM5849 and GM9607 AT cells, respectively, were positive for hRad51 at 24 h (Fig. 7b). hRad51 protein levels are increased in SV40-transformed normal and AT cells relative to those in 180BR and IMR90 primary fibroblasts (Fig. 8a), but the abundance of hRad51 in GM637 and GM9607 cells is unaffected by irradiation (Fig. 8a). Flow cytometry profiles indicated that the majority of AT cells had accumulated in G_2/M at 24 h following irradiation (data not shown), as observed previously (18). Thus, AT cells failed to respond to ionizing radiation with hMre11-hRad50 foci but maintained a distinct and elevated hRad51 IRIF response.

DISCUSSION

Immunofluorescence analysis in situ offers a way to correlate various metabolic processes with the locations of specific proteins and has provided evidence that certain functions may be
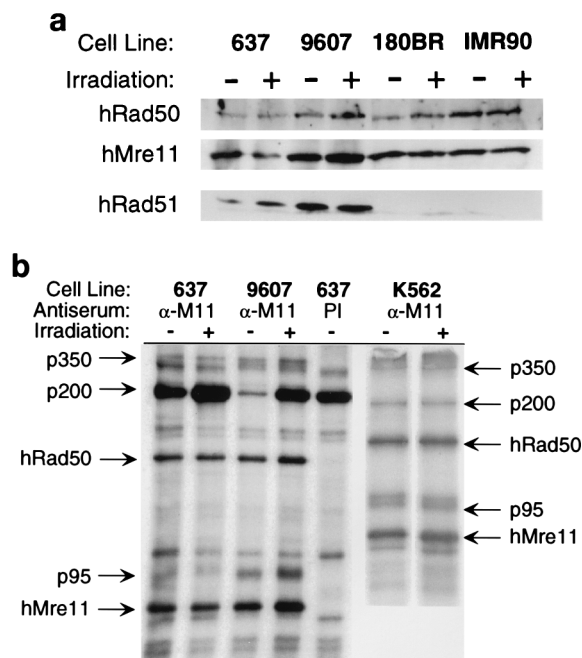

FIG. 8. (a) hMre11, hRad50, and hRad51 expression following treatment with ionizing radiation. Log-phase cells were irradiated or mock irradiated (as indicated) and harvested for immunoblot analysis at 8 h postirradiation. Whole-cell extracts from 2×10^5 cells were loaded in each lane. The same blot was serially probed with the indicated antisera as described in Materials and Methods. 637, GM637, normal SV40-transformed fibroblasts; 9607, GM9607, SV40-transformed AT fibroblasts; 180BR, untransformed DSB repair-deficient fibroblasts; IMR90, untransformed normal fibroblasts. We have shown that hRad51 expression is normal in 180BR and IMR90 cells (data not shown); the abundance of hRad51 in these primary fibroblasts is too low to be detected in this experiment. (b) The hMre11-hRad50 complex is not altered by ionizing radiation. GM637, GM9607, and K562 cells were irradiated or mock irradiated and metabolically labeled with [^{35}S]methionine, as described in Materials and Methods. Extracts were prepared at 8 h postirradiation, immunoprecipitated with anti-hMre11 antiserum (α-hM11) and autoradiographed. Control immunoprecipitations with preimmune serum (PI) were identical for GM637 cells (shown) and GM9607 cells (not shown). Proteins specific to hMre11 immunoprecipitates are labeled as in reference 15. Immunoprecipitates of both preimmune serum and anti-hMre11 antiserum from SV40-transformed fibroblasts contain an abundant 200-kDa nonspecific band that obscures the protein termed p200 (15) (compare to K562 cells). The unirradiated K562 lane has been published previously (15).

GM5849. In GM9607, the percentage of hMre11 IRIF-positive nuclei was similar to that in GM637, but the GM9607 hMre11 foci were atypical in size and fluorescence intensity. This difference presumably reflects the absence of hRad50 in the hMre11 IRIF (data not shown). Importantly, hRad50 and hMre11 are present at normal levels in GM9607, and their abundance is unaffected by irradiation (Fig. 8a). In addition, irradiation does not induce alteration of the apparent stoichiometry of the hMre11-hRad50 complex (Fig. 8b). Approximately 47% of the initial DSBs were unrepaired in irradiated GM9607 cells, compared to less than 1% unrepaired DSBs in irradiated GM637 control cells (Table 1).

Since the AT cell lines we examined were deficient in the hMre11-hRad50 IRIF response, we questioned whether AT cells were also deficient in the hRad51 focus-forming response to ionizing radiation. We used anti-hRad51 antiserum to ex-

regulated by their association with particular sites or structures within the nucleus. Immunofluorescence has been used to describe compartmentalization of nuclear proteins of unknown function into novel focal structures (e.g., PML [16, 79]; polymorphic interphase karyosomal association [PIKA] [65]) and has provided evidence that diverse processes, including DNA replication (27), RNA splicing (20), and DNA repair (23, 48, 58, 76), may be compartmentalized within the nucleus. This experimental approach has also uncovered previously unsuspected roles for certain proteins, such as BRCA1, ATM, and ATR, in meiosis (36, 69).

In this study, we used immunofluorescence to describe the redistribution of hMre11 and hRad50 to discrete foci within the nucleus following DNA damage. We have demonstrated that hRad50 and hMre11 steady-state protein levels are not altered following ionizing radiation or by changes in cell cycle position (Fig. 8a) (15, 45). Therefore, IRIF formation results from changes in the location rather than the abundance of hMre11 or hRad50. The hMre11-hRad50 IRIF response is a dose-dependent, dynamic process. We observed that hMre11 and hRad50 IRIF colocalize, whereas hMre11 and hRad51 foci do not, supporting genetic evidence of their independent roles in DSB repair (59). The formation of hRad50-hMre11 and hRad51 foci is altered in cell lines deficient in the cellular response to DNA damage. These studies suggest that the localization of recombinational DNA repair proteins to discrete nuclear foci is part of the normal DNA damage response.

IRIF formation is dependent upon DSBs. We demonstrated that hMre11-hRad50 foci are specifically induced by DNA DSB-inducing agents (Fig. 1; Table 1). The induction of DNA DSBs by ionizing radiation is linearly dependent upon the radiation dose (43, 53). The number of IRIF per nucleus also increases with dose (Fig. 4), indicating that the number of DNA DSBs initially formed determines the multiplicity of the hMre11-hRad50 IRIF response. Treatment with etoposide, which induces DNA DSBs by trapping topoisomerase II complexes (11, 70), also induced hMre11 foci. Etoposide preferentially induces damage in S and G_2 (12), presumably due to higher expression of topoisomerase II during the S and G_2 phases (25, 28). The number of hMre11 focus-positive nuclei following etoposide treatment corresponded approximately to the percentage of S- and G_2-phase cells in log-phase IMR90 fibroblasts (data not shown). These observations support the interpretation that IRIF formation is dependent upon the induction of DSBs.

This assertion is further supported by the hMre11-hRad50 IRIF response in the DSB repair-deficient cell line 180BR. Ionizing radiation-induced DSBs in 180BR cells are 6- to 10-fold-longer-lived than those in normal cells, and these cells are extremely sensitive to the induction of chromosome aberrations by ionizing radiation ($\geq 45\%$ aberrant metaphases induced by 2 Gy) (3, 4). The molecular defect in this cell line is unknown; however, hMre11 and hRad50 expression and interaction are unaltered in 180BR cells (45). The persistence of unrepaired DSBs in 180BR cells at the time point examined (8 h) (Table 1) thus results in greater numbers of hMre11-hRad50 IRIF in these cells (Fig. 6). Together, our results are consistent with the hypothesis that hMre11-hRad50 foci form following the induction of DSBs and argue that focus formation reflects hMre11-hRad50 function in the normal cellular response to DSBs.

Independent formation of hMre11-hRad50 and hRad51 IRIF. Genetic analyses with *S. cerevisiae* indicate that there is minimal functional overlap in the proteins that mediate homologous recombination (e.g., Rad51) and nonhomologous end joining (e.g., Mre11 and Rad50) (59). Colocalization of hMre11 and hRad50 IRIF (Fig. 2) is consistent with the idea that hMre11 and hRad50 function together in a protein complex during DSB repair (15). hMre11 (and therefore hRad50) IRIF form independently of hRad51 IRIF (Fig. 3), consistent with our finding that hRad51 is not coimmunoprecipable with the hMre11-hRad50 complex (45). Further supporting the functional distinction between hRad51 and hMre11-hRad50 is that hRad51 forms nuclear foci in undamaged cells in the S phase of the cell cycle (69, 75), whereas hMre11-hRad50 foci form only in response to DNA damage. Thus, the focus-forming response of these DSB repair proteins confirms the expectation from *S. cerevisiae* that hMre11-hRad50 and hRad51 mediate distinct functions in DNA metabolism and repair.

IRIF formation is not uniform in the irradiated population. hMre11-hRad50 and hRad51 IRIF do not form in the same nuclei (Fig. 3), indicating that a given cell in the irradiated population is competent to form only one class of focus. This result may suggest that a given irradiated cell is restricted to either homologous recombination or nonhomologous end joining for the repair of DSBs. hMre11-hRad50 or hRad51 IRIF formation may be governed by cell cycle status. Analysis of DSB repair-deficient rodent cells demonstrate the existence of distinct, cell cycle-specific pathways of DSB repair (22, 74). Further, the requirement for a sister chromatid in homologous recombination suggests that this mode of DSB repair would be preferentially utilized in S/G_2. We used asynchronous fibroblast cultures in our experiments. The maximal percentage of hMre11 and hRad50 IRIF-positive cells roughly corresponds to the percentage of cells in G_1 at the time of irradiation (data not shown). Similarly, the percentage of cells in which hRad51 foci are observed roughly corresponds to the initial G_2 population. This correlation is supported by the observation that hRad51 expression is restricted to the S and G_2 phases of the cell cycle (17, 80). Furthermore, recent work has demonstrated that synchronized CHO cells irradiated in G_1 do not form hRad51 IRIF (8a).

The formation of hMre11-hRad50 versus hRad51 foci also appears to be governed by other factors. The percentage of hMre11-hRad50 IRIF-positive nuclei increases as a function of dose (Fig. 4). Dose dependence has similarly been observed for hRad51 foci (23). Thus, IRIF formation depends upon the initial state of the cell, as well as a state that is induced by DNA damage in a dose-dependent fashion.

IRIF formation is altered in AT cells. The *ATM* gene encodes a PI-3-like protein kinase that mediates signal transduction functions upstream of p53 in the DNA damage response (33, 35–37, 66). Loss of ATM signaling function in AT cells impairs cell cycle checkpoint regulation and leads to ionizing radiation sensitivity (52). The radiosensitivity of AT cells cannot be attributed solely to the lack of checkpoint regulation; increased chromosomal damage is observed in cells held in G_0/G_1 (13, 57), and chemically induced cell cycle arrest fails to mitigate the ionizing radiation sensitivity of AT cells (42). These data suggest that ATM controls the processing of chromosomal damage in parallel with its function(s) in cell cycle regulation (46, 52). In this study, we demonstrated that hMre11 and hRad50 IRIF formation is markedly reduced in both AT mutant cell lines we tested but that the hRad51 IRIF response is highly elevated (Fig. 7). Both homologous recombination and nonhomologous end joining are utilized in mammalian DSB repair. If signaling by ATM is important for the function of the hMre11-hRad50 protein complex in the repair of chromosomal damage, the dramatically increased hRad51 response may indicate that DSBs normally repaired by the hMre11-hRad50 protein complex must be repaired by homologous recombination in AT cells. Interestingly, the spontane-

ous rate of homologous recombination in AT cells appears to be significantly increased (47). The data presented here support the hypothesis that the increased sensitivity of AT cells to cell killing and induction of chromosome aberrations following ionizing radiation treatment is at least partially attributable to misregulation of DSB repair processes.

In this regard, it is important that hMre11-hRad50 and hRad51 IRIF are not dependent on p53, as IRIF form in cells with virally inactivated p53 (Fig. 7 and data not shown) (40, 67). This implies a direct link between DSB repair and the ATM signaling pathway that is upstream of p53 cell cycle checkpoint functions. The existence of such a link is also supported by the observation that chromosome aberrations are induced by ionizing radiation in noncycling AT cells (13, 52).

hMre11-hRad50 IRIF are also independent of DNA-PK$_{CS}$, which is implicated in nonhomologous end joining (31). hMre11-hRad50 IRIF were observed in DNA-PK$_{CS}$-null cells (M059J) and DNA-PK$_{CS}$-positive cells (M059K) (data not shown) (2, 39). Further, we have shown that DNA-PK$_{CS}$ and Ku proteins do not coimmunoprecipitate with the hMre11-hRad50 protein complex (45).

The kinetics of IRIF formation resemble those of misrepair and chromosome rearrangement. Previous studies utilizing IMR90 fibroblasts and other repair-proficient cells demonstrate two kinetically distinct modes of DSB repair: a fast component in which >75% of initial DSBs are repaired and a slow component (14, 43, 53). Utilizing a hybridization-based assay, Lobrich et al. determined that the slower-rejoining component consisted of primarily incorrect rejoining events and proceeded over a period of 2 to 48 h postirradiation (43). Premature chromosome condensation assays, in conjunction with fluorescent in situ hybridization, have been used to examine the kinetics of chromosome exchanges and DSB rejoining in irradiated normal fibroblasts. The data suggest that the number of cells with multiple chromosomal exchange events reaches a maximum between 6 to 12 h after irradiation with 10 Gy (10). hMre11-hRad50 IRIF formation follows similar kinetics, with maximal induction at 8 h postirradiation (Fig. 5). In this study, we used neutral comet analyses to confirm that maximal IRIF formation occurs after the majority of DSBs are repaired (Table 1). Thus, whereas the induction of IRIF is dependent upon DSBs, hMre11-hRad50 IRIF may not show a strict relationship with DSBs per se. Given the proposed function of hMre11-hRad50 in recombinational DNA repair and the dependence of IRIF on the prior induction of DNA DSBs, hMre11-hRad50 IRIF may correspond to these exchange or misrepair events.

Conclusion. These studies support the inferred role of the hMre11-hRad50 protein complex in DSB repair. We have established that hMre11-hRad50 IRIF form as part of the normal cellular response to DNA damage. Within an asynchronous culture, cells appear to be committed to the formation of either hMre11-hRad50 or hRad51 IRIF, suggesting a commitment to either nonhomologous end joining or homologous recombination for the repair of DSBs. The hMre11-hRad50 IRIF response is abrogated in AT cells but is unaffected by loss of p53. This may suggest a p53-independent function for ATM that is directly linked to the regulation of recombinational DNA repair. Further assessment of the function of hMre11-hRad50 IRIF awaits the ability to identify DNA DSBs in situ and thereby localize hMre11-hRad50 IRIF to sites of damage. Elucidation of the biochemical activities and composition of the hMre11-hRad50 protein complex will also provide important insight.

REFERENCES

1. **Ajimura, M., S.-H. Leem, and H. Ogawa.** 1993. Identification of new genes required for meiotic recombination in *Saccharomyces cerevisiae*. Genetics **133:**51–66.
2. **Allalunis-Turner, M. J., G. M. Barron, R. S. Day III, K. D. Dobler, and R. Mirzayans.** 1993. Isolation of two cell lines from a human malignant glioma specimen differing in sensitivity to radiation and chemotherapeutic drugs. Radiat. Res. **134:**349–354.
3. **Badie, C., G. Iliakis, N. Foray, G. Alsbeih, B. Cedervall, N. Chavaudra, G. Pantelias, C. Arlett, and E. P. Malaise.** 1995. Induction and rejoining of DNA double-strand breaks and interphase chromosome breaks after exposure to X rays in one normal and two hypersensitive human fibroblast cell lines. Radiat. Res. **144:**26–35.
4. **Badie, C., G. Iliakis, N. Foray, G. Alsbeih, G. E. Pantelias, R. Okayasu, N. Cheong, N. S. Russell, A. C. Begg, C. F. Arlett, and E. P. Malaise.** 1995. Defective repair of DNA double-strand breaks and chromosome damage in fibroblasts from a radiosensitive leukemia patient. Cancer Res. **55:**1232–1234.
5. **Bai, Y., and L. Symington.** 1996. A Rad52 homolog is required for *RAD51*-independent mitotic recombination in *Saccharomyces cerevisiae*. Genes Dev. **10:**2025–2037.
6. **Baker, S. M., A. W. Plug, T. A. Prolla, C. E. Bronner, A. C. Harris, X. Yao, D. M. Christie, C. Monell, N. Arnheim, A. Bradley, T. Ashley, and R. M. Liskay.** 1996. Involvement of mouse *Mlh1* in DNA mismatch repair and meiotic crossing over. Nat. Genet. **13:**336–342.
7. **Bendixen, C., I. Sunjevaric, R. Bauchwitz, and R. Rothstein.** 1994. Identification of a mouse homologue of the *Saccharomyces cerevisiae* recombination and repair gene, *RAD52*. Genomics **23:**300–303.
8. **Bishop, D. K.** 1994. RecA homologs Dmc1 and Rad51 interact to form multiple nuclear complexes prior to meiotic chromosome synapsis. Cell **79:**1081–1092.
8a. **Bishop, D. K.** Personal communication.
9. **Bollag, R. J., A. S. Waldman, and R. M. Liskay.** 1989. Homologous recombination in mammalian cells. Annu. Rev. Genet. **23:**199–225.
10. **Brown, J. M., J. W. Evans, and M. S. Kovacs.** 1993. Mechanism of chromosome exchange formation in human fibroblasts: insights from "chromosome painting." Environ. Mol. Mutagen. **22:**218–224.
11. **Chen, G. L., Y. Yang, T. C. Rowe, B. D. Halligan, K. M. Tewey, and L. F. Liu.** 1984. Nonintercalative antitumor drugs interfere with the breakage-reunion reaction of mammalian DNA topoisomerase II. J. Biol. Chem. **259:**13560–13566.
12. **Chow, K.-C., and W. E. Ross.** 1987. Topoisomerase-specific drug sensitivity in relation to cell cycle progression. Mol. Cell. Biol. **7:**3119–3123.
13. **Cornforth, M. N., and J. S. Bedford.** 1985. On the nature of a defect in cells from individuals with ataxia-telangiectasia. Science **227:**1589–1591.
14. **Cornforth, M. N., and J. S. Bedford.** 1983. X-ray-induced breakage and rejoining of human interphase chromosomes. Science **222:**1141–1143.
15. **Dolganov, G. M., R. S. Maser, A. Novikov, L. Tosto, S. Chong, D. A. Bressan, and J. H. J. Petrini.** 1996. Human Rad50 is physically associated with hMre11: identification of a conserved multiprotein complex implicated in recombinational DNA repair. Mol. Cell. Biol. **16:**4832–4841.
16. **Dyck, J. A., G. G. Maul, W. H. Miller, Jr., J. D. Chen, A. Kakizuka, and R. M. Evans.** 1994. A novel macromolecular structure is a target of the promyelocyte-retinoic acid receptor oncoprotein. Cell **76:**333–343.
17. **Flygare, J., F. Benson, and D. Hellgren.** 1996. Expression of the human RAD51 gene during the cell cycle in primary human peripheral blood lymphocytes. Biochim. Biophys. Acta **1312:**231–236.
18. **Ford, M. D., L. Martin, and M. F. Lavin.** 1984. The effects of ionizing radiation on cell cycle progression in ataxia telangiectasia. Mutat. Res. **125:**115–122.

19. **Friedberg, E. C., G. C. Walker, and W. Siede.** 1995. DNA repair and mutagenesis. ASM Press, Washington, D.C.
20. **Fu, X., and T. Maniatis.** 1990. Factor required for mammalian spliceosome assembly is localized to discrete regions in the nucleus. Nature **343:**437–441.
21. **Game, J. C.** 1993. DNA double strand breaks and the *RAD50-RAD57* genes in *Saccharomyces*. Cancer Biol. **4:**73–83.
22. **Giaccia, A., R. Weinstein, J. Hu, and T. D. Stamato.** 1985. Cell cycle-dependent repair of double-strand DNA breaks in a gamma-ray-sensitive Chinese hamster cell. Somat. Cell Mol. Genet. **11:**485–491.
23. **Haaf, T., E. I. Golub, G. Reddy, C. M. Radding, and D. C. Ward.** 1995. Nuclear foci of mammalian Rad51 recombination protein in somatic cells after DNA damage and its localization in synaptonemal complexes. Proc. Natl. Acad. Sci. USA **92:**2298–2302.
24. **Haber, J. E.** 1992. Exploring the pathways of homologous recombination. Curr. Opin. Cell Biol. **4:**401–412.
25. **Heck, M. M. S., W. N. Hittelman, and W. C. Earnshaw.** 1988. Differential expression of DNA topoisomerases I and II during the eukaryotic cell cycle. Proc. Natl. Acad. Sci. USA **85:**1086–1090.
26. **Houldsworth, J., and M. F. Lavin.** 1980. Effect of ionizing radiation on DNA synthesis in ataxia telangiectasia cells. Nucleic Acids Res. **8:**3709–3720.
27. **Hozak, P., A. B. Hassan, D. A. Jackson, and P. R. Cook.** 1993. Visualization of replication factories attached to a nucleoskeleton. Cell **73:**361–373.
28. **Hsiang, Y.-H., Y.-H. Wu, and L. F. Liu.** 1988. Proliferation-dependent regulation of DNA topoisomerase II in cultured human cells. Cancer Res. **48:**3230–3235.
29. **Iliakis, G.** 1991. The role of DNA double strand breaks in ionizing radiation-induced killing of eukaryotic cells. Bioessays **13:**641–648.
30. **Ivanov, E. L., V. G. Korolev, and F. Fabre.** 1992. *XRS2*, a DNA repair gene of *Saccharomyces cerevisiae*, is needed for meiotic recombination. Genetics **132:**651–664.
31. **Jackson, S. P.** 1996. DNA damage detection by DNA dependent protein kinase and related enzymes. Cancer Surveys **28:**261–279.
32. **Jackson, S. P., and P. A. Jeggo.** 1995. DNA double-strand break repair and V(D)J recombination: involvement of DNA-PK. Trends Biochem. Sci. **20:**412–415.
33. **Jung, M., A. Kondratyev, S. A. Lee, A. Dimtchev, and A. Dritschilo.** 1997. *ATM* gene product phosphorylates IκB-α. Cancer Res. **57:**24–27.
34. **Kanaar, R., C. Troelstra, S. M. A. Swagemakers, J. Essers, B. Smit, J.-H. Franssen, A. Pastink, O. Y. Bezzubova, J.-M. Buerstedde, B. Clever, W.-D. Heyer, and J. H. J. Hoeijmakers.** 1996. Human and mouse homologs of the *Saccharomyces cerevisiae RAD54* DNA repair gene: evidence for functional conservation. Curr. Biol. **6:**828–838.
35. **Kastan, M. B., Q. Zhan, W. S. El-Diery, F. Carrier, T. Jacks, W. V. Walsh, B. S. Plunkett, B. Vogelstein, and A. J. Fornace.** 1992. A mammalian cell cycle checkpoint pathway utilizing p53 and *GADD45* is defective in ataxia-telangiectasia. Cell **71:**587–597.
36. **Keegan, K. S., D. A. Holtzman, A. W. Plug, E. R. Christenson, E. E. Brainerd, G. Flaggs, N. J. Bentley, E. M. Taylor, M. S. Meyn, S. B. Moss, A. M. Carr, T. Ashley, and M. F. Hoekstra.** 1996. The Atr and Atm protein kinases associate with different sites along meiotically pairing chromosomes. Genes Dev. **10:**2423–2437.
37. **Khanna, K. K., H. Beamish, J. Yan, K. Hobson, R. Williams, I. Dunn, and M. F. Lavin.** 1995. Nature of G1/S cell cycle checkpoint defect in ataxia-telangiectasia. Oncogene **11:**609–618.
38. **Lavin, M. F., K. K. Khanna, H. Beamish, B. Teale, K. Hobson, and D. Watters.** 1994. Defect in radiation signal transduction in ataxia-telangiectasia. Int. J. Radiat. Biol. **66:**S151–S156.
39. **Lees-Miller, S. P., R. Godbout, D. W. Chan, M. Weinfeld, R. S. Day III, G. M. Barron, and J. Allalunis-Turner.** 1995. Absence of p350 subunit of DNA-activated protein kinase from a radiosensitive human cell line. Science **267:**1183–1185.
40. **Levine, A. J.** 1990. Tumor suppressor genes. Bioessays **12:**60–66.
41. **Li, M.-J., M. Peakman, E. I. Golub, G. Reddy, D. C. Ward, C. M. Radding, and N. Maizels.** 1996. Rad51 expression and localization in B cells carrying out class switch recombination. Proc. Natl. Acad. Sci. USA **93:**10222–10227.
42. **Little, J. B., and H. Nagasawa.** 1985. Effect of confluent holding on potentially lethal damage repair, cell cycle progression, and chromosomal aberrations in human normal and ataxia-telangiectasia fibroblasts. Radiat. Res. **101:**81–93.
43. **Lobrich, M., B. Rydberg, and P. K. Cooper.** 1995. Repair of x-ray induced DNA double strand breaks in specific Not I restriction fragments in human fibroblasts: joining of correct and incorrect ends. Proc. Natl. Acad. Sci. USA **92:**12050–12054.
44. **Lukacsovich, T., D. Yang, and A. S. Waldman.** 1994. Repair of a specific double-strand break generated within a mammalian chromosome by yeast endonuclease I-SceI. Nucleic Acids Res. **22:**5649–5657.
45. **Maser, R. S., and J. H. J. Petrini.** 1997. Unpublished data.
46. **Meyn, M. S.** 1995. Ataxia-telangiectasia and cellular responses to DNA damage. Cancer Res. **55:**5991–6001.
47. **Meyn, M. S.** 1993. High spontaneous rates of intrachromosomal recombination in ataxia-telangiectasia. Science **260:**1327–1330.
48. **Miura, M., M. Domon, T. Sasaki, S. Kondo, and Y. Takasaki.** 1992. Two types of proliferating cell nuclear antigen (PCNA) complex formation in quiescent normal and xeroderma pigmentosum group A fibroblasts following ultraviolet light (uv) irradiation. Exp. Cell Res. **201:**541–544.
49. **Montecucco, A., E. Savini, F. Weighardt, R. Rossi, G. Ciarrocchi, A. Villa, and G. Biamonti.** 1995. The N-terminal domain of human DNA ligase I contains the nuclear localization signal and directs the enzyme to sites of DNA replication. EMBO J. **14:**7379–7386.
50. **Moore, J. K., and J. E. Haber.** 1996. Cell cycle and genetic requirements of two pathways of nonhomologous end-joining repair of double-strand breaks in *Saccharomyces cerevisiae*. Mol. Cell. Biol. **16:**2164–2173.
51. **Morgan, W. F., J. P. Day, M. I. Kaplan, E. M. McGhee, and C. L. Limoli.** 1996. Genomic instability induced by ionizing radiation. Radiat. Res. **146:**247–258.
52. **Murnane, J. P.** 1995. Cell cycle regulation in response to DNA damage in mammalian cells: a historical perspective. Cancer Metastasis Rev. **14:**17–29.
53. **Nevaldine, B., J. A. Longo, G. A. King, M. Vilenchik, R. H. Sagerman, and P. J. Hahn.** 1993. Induction and repair of DNA double-strand breaks. Radiat. Res. **133:**370–374.
54. **Olive, P. L., J. P. Banath, and R. E. Durand.** 1990. Detection of etoposide resistance by measuring DNA damage in individual Chinese hamster cells. J. Natl. Cancer Inst. **82:**779–783.
55. **Olive, P. L., D. Wlodek, and J. P. Banath.** 1991. DNA double-strand breaks measured in individual cells subjected to gel electrophoresis. Cancer Res. **51:**4671–4676.
56. **Painter, R. B.** 1981. Radioresistant DNA synthesis: an intrinsic feature of ataxia telangiectasia. Mutat. Res. **84:**183–190.
57. **Pandita, T. K., and W. N. Hittelman.** 1992. Initial chromosome damage but not DNA damage is greater in ataxia telangiectasia cells. Radiat. Res. **130:**94–103.
58. **Park, M. S., J. A. Knauf, S. H. Pendergrass, C. H. Coulon, G. F. Strniste, B. L. Marrone, and M. A. MacInnes.** 1996. Ultraviolet-induced movement of the human DNA repair protein, *Xeroderma pigmentosum* type G, in the nucleus. Proc. Natl. Acad. Sci. USA **93:**8368–8373.
59. **Petrini, J. H. J., D. A. Bressan, and M. S. Yao.** 1997. The *RAD52* epistasis group in mammalian double strand break repair. Semin. Immunol. **9:**181–188.
60. **Petrini, J. H. J., M. E. Walsh, C. Di Mare, J. R. Korenberg, X.-N. Chen, and D. T. Weaver.** 1995. Isolation and characterization of the Human MRE11 homologue. Genomics **29:**80–86.
61. **Planchon, S. M., S. Wuerzberger, B. Frydman, D. T. Witiak, P. Hutson, D. R. Church, G. Wilding, and D. A. Boothman.** 1995. β-Lapachone-mediated apoptosis in human promyelocytic leukemia (HL-60) and human prostate cancer cells: a p53-independent response. Cancer Res. **55:**3706–3711.
62. **Plug, A. W., J. Xu, G. Reddy, E. I. Golub, and T. Ashley.** 1996. Presynaptic association of Rad51 protein with selected sites in meiotic chromatin. Proc. Natl. Acad. Sci. USA **93:**5920–5924.
63. **Roeder, G. S.** 1995. Sex and the single cell: meiosis in yeast. Proc. Natl. Acad. Sci. USA **92:**10450–10456.
64. **Roth, D. B., and J. H. Wilson.** 1988. Illegitimate recombination in mammalian cells, p. 621–654. *In* R. Kucherlapati and G. R. Smith (ed.), Genetic recombination. American Society for Microbiology, Washington, D.C.
65. **Saunders, W. S., C. A. Cooke, and W. C. Earnshaw.** 1991. Compartmentalization within the nucleus: discovery of a novel subnuclear region. J. Cell Biol. **115:**919–931.
66. **Savitsky, K., A. Bar-Shira, S. Gilad, G. Rotman, Y. Ziv, L. Vanagaite, D. A. Tagle, S. Smith, T. Uziel, S. Sfez, M. Ashkenazi, I. Pecker, M. Frydman, R. Harnik, S. R. Patanjali, A. Simmons, G. A. Clines, A. Sartiel, R. A. Gatti, L. Chessa, O. Sanal, M. F. Lavin, N. G. J. Jaspers, A. M. R. Taylor, C. F. Arlett, T. Miki, S. M. Weissman, M. Lovett, F. S. Collins, and Y. Shiloh.** 1995. A single ataxia telangiectasia gene with a product similar to PI-3 kinase. Science **268:**1749–1753.
67. **Scheffner, M., K. Munger, J. C. Byrne, and P. M. Howley.** 1991. The state of the p53 and retinoblastoma genes in human cervical carcinoma cell lines. Proc. Natl. Acad. Sci. USA **88:**5523–5527.
68. **Schiestl, R. H., J. Zhu, and T. D. Petes.** 1994. Effect of mutations in genes affecting homologous recombination on restriction enzyme-mediated and illegitimate recombination in *Saccharomyces cerevisiae*. Mol. Cell. Biol. **14:**4495–4500.
69. **Scully, R., J. Chen, A. Plug, Y. Xiao, D. Weaver, J. Feunteun, T. Ashley, and D. M. Livingston.** 1997. Association of BRCA1 with Rad51 in mitotic and meiotic cells. Cell **88:**265–275.
70. **Sestili, P., F. Cattabeni, and O. Cantoni.** 1995. Simultaneous determination of DNA double strand breaks and DNA fragment size in cultured mammalian cells exposed to hydrogen peroxide/histidine or etoposide with CHEF electrophoresis. Carcinogenesis **16:**703–706.
71. **Shen, Z., K. Denison, R. Lobb, J. M. Gatewood, and D. J. Chen.** 1995. The human and mouse homologs of the yeast RAD52 gene: cDNA cloning, sequence analysis, assignment to human chromosome 12p12.2-p13, and mRNA expression in mouse testis. Genomics **25:**199–206.
72. **Shinohara, A., H. Ogawa, Y. Matsuda, N. Ushio, K. Ikeo, and T. Ogawa.** 1993. Cloning of the human, mouse, and fission yeast recombination genes homologous to *RAD51* and *recA*. Nat. Genet. **4:**239–243.

73. **Shinohara, A., and T. Ogawa.** 1995. Homologous recombination and the roles of double-strand breaks. Trends Biochem. Sci. **20:**387–390.
74. **Stamato, T. D., R. Weinstein, A. Giaccia, and L. Mackenzie.** 1983. Isolation of cell cycle-dependent gamma ray-sensitive Chinese hamster ovary cell. Somatic Cell Genet. **9:**165–173.
75. **Tashiro, S., N. Kotomura, A. Shinohara, K. Tanaka, K. Ueda, and N. Kamada.** 1996. S phase specific formation of the human Rad51 protein nuclear foci in lymphocytes. Oncogene **12:**2165–2170.
76. **Toschi, L., and R. Bravo.** 1987. Changes in cyclin/proliferating cell nuclear antigen distribution during DNA repair synthesis. J. Cell Biol. **107:**1623–1628.
77. **Tsukamoto, Y., J. Kato, and H. Ikeda.** 1996. Effects of mutations of *RAD50*, *RAD51*, *RAD52*, and related genes on illegitimate recombination in *Saccharomyces cerevisiae*. Genetics **142:**383–391.
78. **Weaver, D. T.** 1995. What to do at an end: DNA double-strand break repair. Trends Genet. **11:**388–392.
79. **Weis, K., S. Rambaud, C. Lavau, J. Jansen, T. Carvalho, M. Carmo-Fonseca, A. Lamond, and A. Dejean.** 1994. Retinoic acid regulates aberrant nuclear localization of PML-RARα in acute promyelocytic leukemia cells. Cell **76:**345–356.
80. **Yamamoto, A., T. Taki, H. Yagi, T. Habu, K. Yoshida, Y. Yoshimura, K. Yamamoto, A. Matsushiro, Y. Nishimune, and T. Morita.** 1996. Cell cycle-dependent expression of the mouse *Rad51* gene in proliferating cells. Mol. Gen. Genet. **251:**1–12.